Progressive and Biased Divergent Evolution Underpins the Origin and Diversification of Peridinin Dinoflagellate Plastids

Richard G. Dorrell,^{*,1} Christen M. Klinger,^{†,2} Robert J. Newby,^{3,†} Erin R. Butterfield,^{4,5} Elisabeth Richardson,² Joel B. Dacks,² Christopher J. Howe,⁶ Ellen R. Nisbet,⁶ and Chris Bowler¹ ¹Ecole Normale Supérieure, PSL Research University, Institut de Biologie de l'Ecole Normale Supérieure (IBENS), CNRS UMR 8197, INSERM U1024, Paris, France ²Department of Cell Biology, University of Alberta, Edmonton, AB, Canada ³Department of Biology, Middle Tennessee State University, Murfreesbro, TN ⁴Department of Biochemistry, Pennsylvania State University, State College, PA ⁵School of Life Sciences, University of Dundee, Dundee, Scotland

⁶Department of Biochemistry, University of Cambridge, Cambridge, United Kingdom

[†]These authors contributed equally to this work.

*Corresponding author: E-mail: dorrell@biologie.ens.fr

Associate editor: James McInerney

Abstract

Dinoflagellates are algae of tremendous importance to ecosystems and to public health. The cell biology and genome organization of dinoflagellate species is highly unusual. For example, the plastid genomes of peridinin-containing dinoflagellates encode only a minimal number of genes arranged on small elements termed "minicircles". Previous studies of peridinin plastid genes have found evidence for divergent sequence evolution, including extensive substitutions, novel insertions and deletions, and use of alternative translation initiation codons. Understanding the extent of this divergent evolution has been hampered by the lack of characterized peridinin plastid sequences. We have identified over 300 previously unannotated peridinin plastid mRNAs from published transcriptome projects, vastly increasing the number of sequences available. Using these data, we have produced a well-resolved phylogeny of peridinin plastid lineages, which uncovers several novel relationships within the dinoflagellates. This enables us to define changes to plastid sequences that occurred early in dinoflagellate evolution, and that have contributed to the subsequent diversification of individual dinoflagellate clades. We find that the origin of the peridinin dinoflagellates was specifically accompanied by elevations both in the overall number of substitutions that occurred on plastid sequences, and in the Ka/Ks ratio associated with plastid sequences, consistent with changes in selective pressure. These substitutions, alongside other changes, have accumulated progressively in individual peridinin plastid lineages. Throughout our entire dataset, we identify a persistent bias toward non-synonymous substitutions occurring on sequences encoding photosystem I subunits and stromal regions of peridinin plastid proteins, which may have underpinned the evolution of this unusual organelle.

Key words: alveolates, algae, poly(U) tail, chloroplast genomes, MMETSP.

Introduction

Dinoflagellates are eukaryotes with immense ecological and evolutionary importance. They include photosynthetic, heterotrophic, mixotrophic, and parasitic representatives (Dorrell and Howe 2015). The photosynthetic species are a major component of plankton communities in marine and freshwater environments (Leterme et al. 2006; de Vargas et al. 2015), and include causative agents of harmful algal blooms (*Protoperidinium, Ceratium*) (Hallegraeff 2010; Hinder et al. 2012), and the symbionts of corals (*Symbiodinium*) and of marine protozoa (*Pelagodinium, Brandtodinium*) (Siano et al. 2010; Probert et al. 2014). The non-photosynthetic species include parasites of marine invertebrates (*Hematodinium*, Syndiniales, and ellobiopsids) (Gornik et al. 2012), and bioluminescent phagotrophs (*Noctiluca*) (Nakamura 1998). Dinoflagellates are members of the alveolates, a group that additionally contains important laboratory model species (ciliates such as *Paramecium* and *Tetrahymena*), pathogens of terrestrial and marine animals (e.g., the apicomplexan parasites *Plasmodium* and *Toxoplasma*, and the mollusc pathogen *Perkinsus*), and other ecologically significant heterotrophs (ciliates and gregarines). Two other photosynthetic alveolates have been described (the "chromerids" *Chromera* and *Vitrella*), both of which are closely related to the apicomplexans, and serve as model organisms for understanding the origins of parasitism in this lineage (Janouskovec et al. 2010; Dorrell and Howe 2015).

Dinoflagellates are renowned for their unusual and distinctive cell biology (Lin 2011; Wisecaver and Hackett 2011; Dorrell and Howe 2015). Unlike those of all other studied

© The Author 2016. Published by Oxford University Press on behalf of the Society for Molecular Biology and Evolution. This is an Open Access article distributed under the terms of the Creative Commons Attribution Non-Commercial License (http://creativecommons.org/licenses/by-nc/4.0/), which permits non-commercial re-use, distribution, and reproduction in any medium, provided the original work is properly cited. For commercial re-use, please contact journals.permissions@oup.com



eukaryotes, dinoflagellate chromosomes are maintained in a permanently condensed state, and do not principally utilise histones for DNA packaging (Gornik et al. 2012). The mitochondrial genomes of dinoflagellates and apicomplexans are highly reduced, and several otherwise well-conserved subunits of the ATP synthase complex have not been documented in any dinoflagellate (Butterfield et al. 2013; Janouškovec et al. 2013).

One of the oddest traits of dinoflagellate cell biology is their possession of unusual plastids. While all other major eukaryotic groups are either non-photosynthetic, or contain only one plastid lineage, at least four and potentially as many as seven phylogenetically distinct plastid lineages have been documented across the dinoflagellates (Janouskovec et al. 2010; Dorrell and Howe 2015). The majority of photosynthetic dinoflagellates possess plastids that contain the light harvesting pigment peridinin (Haxo et al. 1976). These "peridinin plastids" are most likely of red algal origin, although the exact endosymbiotic events through which they originated remain debated (Keeling 2010; Ševčíková et al. 2015). Phylogenetic studies have indicated that the peridinin plastid was present in a common ancestor of dinoflagellates, chromerids, and apicomplexans, and that the alternative plastids found in some dinoflagellates have originated through serial endosymbiosis (Janouskovec et al. 2010; Dorrell and Howe 2015).

The genome of the peridinin plastid is the smallest known from a photosynthetic plastid, retaining only 12 protein-coding genes (Barbrook et al. 2014; Mungpakdee et al. 2014), plus ribosomal RNA and some transfer RNA genes (Barbrook et al. 2006; Nelson et al. 2007). The protein coding genes solely encode core subunits of the photosynthetic electron transport machinery, comprising genes encoding six subunits of photosystem II (psbA, psbB, psbC, psbD, psbE, psbI), and two subunits each of photosystem I (psaA, psaB), cytochrome b_6/f (petB, petD), and plastid ATP synthase (atpA, atpB). These genes are located on small elements termed "minicircles" (of 1,600-6,600-bp length) (Zhang et al. 1999; Nelson and Green 2005) and "microcircles" (of 400–600-bp length) (Nisbet et al. 2004). Minicircles typically contain single genes, although minicircles that contain no genes (Nisbet et al. 2004; Nelson et al. 2007), or combinations of multiple genes have also been identified in multiple dinoflagellate species (Hiller 2001; Nisbet et al. 2004; Nelson et al. 2007). All other genes of unambiguously plastid origin that have been documented in peridinin dinoflagellates are located in the nucleus (Morse et al. 1995; Bachvaroff et al. 2004; Mungpakdee et al. 2014). Some minicircles contain sizeable open reading frames of unknown function that are unique to dinoflagellates (Barbrook et al. 2001, 2006; Nisbet et al. 2004). It has been proposed that some peridinin plastids contain genes encoding ribosomal proteins (rpl28, rpl33) and iron-sulfur cluster biogenesis factors (ycf16, ycf24), which were acquired by horizontal gene transfer from non-photosynthetic bacteria, although whether these sequences are genuinely plastidencoded remains controversial (Moszczynski et al. 2012; Dorrell and Howe 2015).

Alongside the extreme level of reduction observed in the peridinin plastid genome, the transcript sequences produced in peridinin plastids are highly unusual. This is in part due to the unusual transcript processing machinery associated with peridinin plastids, which includes (in some species) extensive in-frame sequence editing (Zauner et al. 2004; Dorrell and Howe 2015) and (in all documented species) the addition of a 3' poly(U) tail to plastid mRNAs (Wang and Morse 2006; Barbrook et al. 2012), which contrast with the 3' poly(A) tail and 5' spliced-leader sequences added to transcripts in dinoflagellate nuclei (Zhang et al. 2007). In addition, individual genes within peridinin plastids are highly divergent from orthologous from other plastid lineages (Shalchian-Tabrizi et al. 2006; Pochon et al. 2014). The genes located in peridinin plastids frequently contain extensive sequence substitutions (Barbrook et al. 2014) and in-frame insertions and deletions (Barbrook et al. 2006, 2014), have unusual codon usage preferences (Inagaki et al. 2004; Bachvaroff et al. 2006) and use a range of alternative translation initiation codons in addition to ATG (ATA, ATT, GTA, TTG) (Zhang et al. 1999; Barbrook et al. 2014).

This project was conceived to investigate the timing and extent of the divergent sequence evolution in peridinin plastids. It is broadly agreed that application of poly(U) tails to plastid transcripts is an ancestral feature of peridinin dinoflagellates, and it has been proposed that the fragmentation of the peridinin plastid genome into minicircles, and the reduction of the plastid genome to a minimal protein-coding gene set, are likewise ancestral (Janouskovec et al. 2010; Dorrell et al. 2014; Dorrell and Howe 2015). However, it is not known when other divergent evolutionary events occurred in peridinin plastids. This has in part been due to the lack of available sequence information, with essentially complete plastid coding sequences previously available only for Amphidinium carterae (Nisbet et al. 2004), and for two strains of Symbiodinium (Clade C3, and Clade Mf) (Barbrook et al. 2014; Mungpakdee et al. 2014). In addition, the phylogenetic relationships within the peridinin dinoflagellates remain poorly resolved. While Amphidinium is agreed to diverge at the base of the peridinin dinoflagellates, the branching order of other lineages remains debated (Hoppenrath and Leander 2010; Bachvaroff et al. 2014; Gavelis et al. 2015). We wished to generate a robust phylogeny of extant peridinin dinoflagellate lineages, and use this phylogeny to answer three questions: (1) which of the divergent features associated with peridinin plastid sequences are likely to have originated in an ancestor to all species studied; (2) to what extent and in which dinoflagellate lineages have divergent plastid evolution events occurred more recently, and (3) whether there are any consistent trends across the dinoflagellates in terms of which plastid-encoded proteins, or regions of plastid-encoded proteins, are the most divergent, extending from their common ancestor through to extant species.

We present a taxonomically detailed reconstruction of the evolution of peridinin plastid sequences. We have focused on identifying novel plastid transcripts, which allows us to assess the composite effects of divergent gene evolution and transcript editing on peridinin plastid sequences (Zauner et al. 2004; Dorrell and Howe 2015). We have annotated over 300 new peridinin plastid sequences from published transcriptome resources, and demonstrate that the twelve photosystem genes previously identified in peridinin plastids (Mungpakdee et al. 2014; Dorrell and Howe 2015) probably represent the complete protein-coding component of the plastid genome of a common ancestor of all extant peridinin dinoflagellates. We have used these sequences to generate a well-resolved phylogeny of peridinin plastids, uncovering novel evolutionary relationships between the major dinoflagellate lineages, and have used this phylogeny to determine when different divergent evolutionary events have occurred in peridinin plastids. To disentangle the different factors that have underpinned this unusual sequence evolution, we have calculated substitution rates, and Ka/Ks ratios [also referred to as dN/dS, and defined as the relative enrichment in nonsynonymous substitutions, Ka, to synonymous substitutions, Ks, over a particular sequence, which provides an indicator of the strength of selective pressure (Yang and Bielawski 2000; Hurst 2002)] for each dinoflagellate species and each residue of each plastid-encoded protein studied.

We show that the origin of the peridinin plastid was specifically marked by an elevation in substitution rates and in Ka/Ks ratios, consistent with changes in selection pressure in the dinoflagellate common ancestor. We additionally show that these and other divergent features, such as in-frame insertions and alternative translation initiation codons, have continued to evolve progressively in individual dinoflagellate clades. Finally, we show that in both the common ancestor of all studied peridinin dinoflagellates and in extant species, elevated Ka/Ks ratios are concentrated on genes encoding photosystem I subunits, and codons encoding stromal-facing residues of plastid proteins. This may suggest that specific changes to dinoflagellate physiology have driven the divergent evolution of the peridinin plastid. Ultimately, our study provides valuable insights into the evolutionary history of this unusual plastid lineage, from its very origins and through its subsequent diversification.

Results

Annotation of New Peridinin Plastid Sequences From Transcriptome Data

Identification of Plastid Sequences

New dinoflagellate orthologues of the 12 protein-coding genes (atpA, atpB, petB, petD, psaA, psaB, psbA, psbB, psbC, psbD, psbE, and psbI) previously found to be retained in peridinin plastids (Howe et al. 2008; Barbrook et al. 2014; Mungpakdee et al. 2014) were identified in the NCBI EST library, and transcriptome libraries within the Marine Sequencing Microeukaryote Transcriptome Project (MMETSP) (Keeling et al. 2014). A total of 381 sequences were identified, 364 of which had no previously annotated equivalents (fig. 1; supplementary table S1, Supplementary Material online). The majority (348) of the novel sequences were identified from transcripts within the MMETSP libraries, with only a few sequences (16) identifiable from EST libraries located in NCBI (fig. 1). Sequences of plausible plastid origin were identified in all but a few peridinin dinoflagellate MMETSP libraries, with a minimum of 15 novel orthologues found for each gene studied (supplementary table S1,

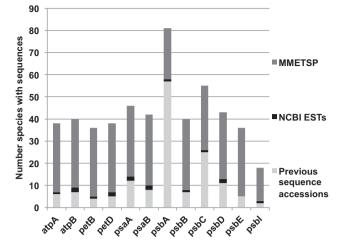


FIG. 1. New peridinin plastid coding sequences identified from transcriptome libraries. This graph shows the number of peridinin dinoflagellates for which sequences of each of the 12 protein-coding genes present in peridinin plastids have been identified, both previously, and from the data presented in this study. Sequences are only counted if they are >200-bp length (for *atpA*, *atpB*, *psaA*, *psaB*, *psbA*, *psbB*, *psbC*, and *psbD*), >100 bp (for *petB*, *petD*, and *psbE*), or > 50 bp (for *psb*).

Supplementary Material online), and complete sets of protein-coding plastid genes identified for 13 new dinoflagellate species in addition to the three already characterized (Howe et al. 2008; Barbrook et al. 2014; Mungpakdee et al. 2014).

Novel Sequences Are of Probable Plastid Origin

Uninterrupted poly(T) stretches of 4 bp or longer were detected on the 3' end of half (191/381) of the novel dinoflagellate sequences, consistent with the presence of the poly(U) tails associated with dinoflagellate plastid transcripts (supple mentary fig. S1 and table S1, Supplementary Material online). Across the entire dataset, only one sequence was found that terminated in a possible 3' poly(A) tail, and none contained evidence of 5' spliced-leader sequences, or plausible tripartite targeting sequences (consisting of a signal peptide, ASAFAPdelimited transit peptide, and a downstream hydrophobic region), as are associated with nucleus-encoded, plastid-targeted proteins in peridinin dinoflagellates (Nassoury and Morse 2005; Zhang et al. 2007) (supplementary table S1, Supplementary Material online).

Limited Additional Coding Sequences in Peridinin Plastids The entire assembled transcriptome dataset was screened for further transcripts that might originate from peridinin plastids. We could not find convincing evidence for any further genes that are plastid-encoded in other non-dinoflagellate lineages, and might still be plastid-encoded within individual dinoflagellates, beyond the 12 photosystem genes previously documented (supplementary fig. S2 and supplementary re sults, Section 1, Supplementary Material online). The entire dataset was additionally searched for homologues of the four plastid genes (*rpl28, rpl33, ycf16, ycf24*) proposed to have been

gained by horizontal transfer from bacteria into specific peridinin plastids (Moszczynski et al. 2012). A total of 148 new sequences were identified and inspected using single-gene phylogenies. While the original Pyrocystis lunula and Ceratium horridum sequences grouped with Bacteroidetes, none of the homologues within this dataset did: instead, the majority resolved as a monophyletic group and all grouped either within, or as sister-groups to, other plastid or cyanobacterial lineages, with robust (>90%) bootstrap support (supplementary figs. S3–S6, Supplementary Material online). None of the rpl28, rpl33, ycf16 or ycf24 transcript sequences identified in this study possessed a 3' poly(U) tail (supplementary table S1, Supplementary Material online); however, many contained 3' poly(A) tails, spliced-leader sequences (supplementary table S1, Supplementary Material online), and tripartite plastid targeting sequences (supplemen tary fig. S7, Supplementary Material online), consistent with a nuclear origin.

Homologues of the four novel open reading frames previously identified on minicircles located in the A. carterae plastid (Barbrook and Howe 2000; Dorrell and Howe 2015) were searched for across the entire transcript dataset. Only equivalents of A. carterae ORF1, ORF2 and ORF3 were detected, and these were limited to the related species Amphidinium massartii (supplementary fig. S8, panel A, Supplementary Material online). The ORF-like sequences identified in A. massartii were highly divergent from those of A. carterae, with only 46% (ORF1), 32% (ORF2), and 33% (ORF3) identities shared between sequences from the two species, compared with (e.g.) 97% sequence conservation between the psbD sequences from each species (supplementary fig. S8, panel A, Supplementary Material online). We could find only limited evidence for the presence of additional conserved polyuridylylated transcripts that might correspond to novel plastid ORFs within the dataset (supplementary fig. S8 and supple mentary results, Section 1, Supplementary Material online).

Reconstruction of Phylogenetic Relationships Between Peridinin Dinoflagellates

A concatenated protein alignment (3,410 amino acids, average 72.7% pairwise identities) was generated, consisting of the twelve plastid sequences studied, for each of the dinoflagellates present in MMETSP, and a reference set of fifteen nondinoflagellate (supplementary species table S3. Supplementary Material online). Bayesian and Maximum Likelihood trees were generated from this alignment (fig. 2; supplementary table S4, Supplementary Material online). Two phylogenetically distinct sets of plastid sequences were identified for clade A Symbiodinium, one of which resolved with other Symbiodinium species, and the other as a sister group to A. carterae, which presumably represents a contamination within the Symbiodinium A MMETSP library (fig. 2; supplementary table S1, Supplementary Material online).

Consistent with previous data, *Amphidinium* was identified as the earliest diverging peridinin dinoflagellate genus (fig. 2) (Dorrell and Howe 2015; Gavelis et al. 2015). Following *Amphidinium*, the next most basal dinoflagellates were *Togula jolla*, and a clade consisting of Prorocentrales,

Peridiniales, and the (previously Suessialean) species *Pelagodinium beii*, which diverged from a clade consisting of Gonyaulacales, Suessiales, and the (previously Peridinialean) genus *Heterocapsa*, with moderate to robust support (in Bayesian analysis, >60% in ML trees) (fig. 2). Identical (supple mentary fig. S9, Supplementary Material online) or nearly identical (supplementary fig. S10, Supplementary Material online) topologies to the original tree were obtained in trees calculated from alignments from which long branches, fast evolving sites, or individual plastid genes had been removed (supplementary results, Section 2, Supplementary Material online), suggesting that the initial tree topology was largely accurate.

Dinoflagellate-Wide Changes in Plastid Sequence Composition

Changes in Plastid GC Content May Have Occurred Before the Radiation of the Dinoflagellates

The first, second, and third position GC content were compared across a 4,478-nt gap-free alignment of six plastid genes (psaA, psaB, psbA, psbB, psbC, and psbD), for each of the dinoflagellates studied, and all of the non-dinoflagellate species previously used for the multigene phylogeny (fig. 2). Elevated GC contents were observed at third codon positions in many of the dinoflagellates compared to non-dinoflagellate previously used (supplementary species fig. S11, Supplementary Material online). These included third position GC content values of >35% in three of the earliest diverging dinoflagellate clades (supplementary fig. S11, Supplementary Material online; Amphidinium GC[3] = 39. 6-49.6%, Peridiniales GC[3]=29.8-40.9%, Prorocentrales GC[3]= 31.7-39.5%). However, the chromerid Vitrella brassicaformis, which forms the closest sister-group to the dinoflagellates within the multigene tree (fig. 2), also has a high third position GC content (supplementary fig. S11, Supplementary Material online; 46.9%), so it is possible that this GC enrichment is not specific to dinoflagellates.

Limited Changes to Plastid Translation in the Dinoflagellate Ancestor

Across the entire 4,478-nt gap-free plastid alignment, 18 codons occurred with lower frequency (and 19 codons with higher frequency) in dinoflagellates compared to nondinoflagellate species (one-way ANOVA, P < 0.05; supplemen tary table S5 and fig. S12, Supplementary Material online). Ten amino acids were likewise found to occur with lower frequency, and five with higher frequency, in dinoflagellates (one-way ANOVA, P < 0.05; supplementary table S5 and fig. S12, Supplementary Material online) over this alignment, as inferred by a standard translation table. We could not identify any convincing evidence for changes to plastid translation tables within the dinoflagellates (supplementary table S6 and fig. S13; supplementary results, Section 3, Supplementary Material online).

A much smaller number of codons were found to have undergone specific de-enrichments (6) or enrichments (8; chi-squared test, P < 0.05; supplementary table S5 and

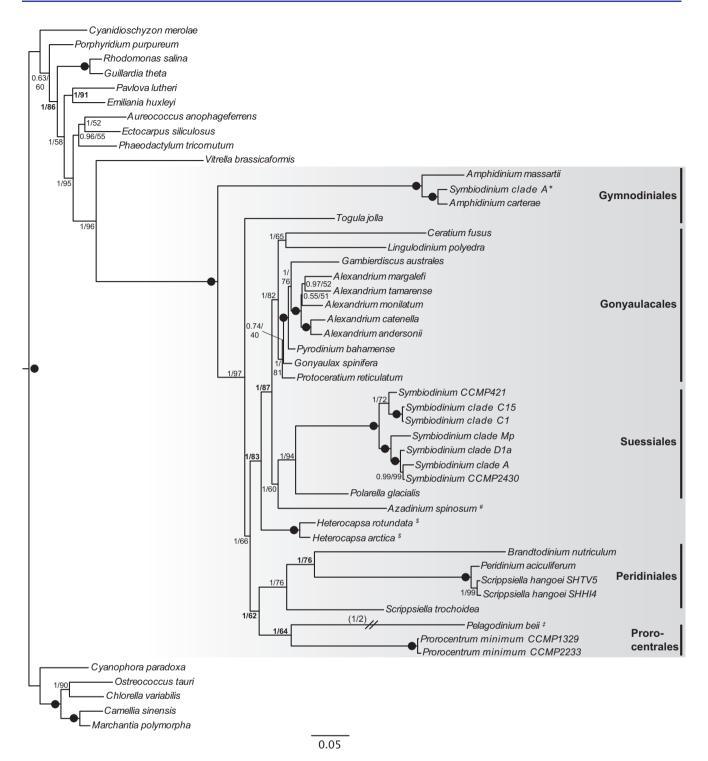


Fig. 2. Multigene protein phylogeny of peridinin dinoflagellates. This figure shows the Bayesian obtained for the 48 species \times 3,410 aa alignment of the 12 proteins that are plastid-encoded in peridinin dinoflagellates. Filled circles at each node indicate support with a posterior probability of 1.0 (for Bayesian inference) and 100% bootstrap values (for RAxML); elsewhere, support values for each node are given in the format (MrBayes/ RAxML). The branch leading to *P. beii* (marked with double crossed lines) has been reduced to half its true length (true length 0.463, displayed length 0.232) to accommodate the branch within the figure. Two phylogenetically distinct populations of sequences identified from the Clade A *Symbiodinium* library are shown, one grouping with other *Symbiodinium* sequences, and the other (asterisked) within *Amphidinium*. Dinoflagellate orders (Gymnodiniales, Gonyaulacales, Peridiniales, Suessiales, and Prorocentrales) are labeled on the diagram. Species that do not resolve with other members of the same order are individually labeled, as follows: # (*Azadinium spinosum*), previously assigned to Gonyaulacales but identified here as a sister group to the Suessiales; \$ (*Heterocapsa* sp.), assigned to Peridiniales but identified here as a sister group to Suessiales but identified here as a sister group to Suessiales but identified here as a sister group to Suessiales but identified here as a sister group to Suessiales but identified here as a sister group to Suessiales but identified here as a sister group to Suessiales but identified here as a sister group to Suessiales but identified here as a sister group to Suessiales but identified here as a sister group to Suessiales but identified here as a sister group to Suessiales but identified here as a sister group to Suessiales but identified here as a sister group to Suessiales but identified here as a sister group to Suessiales but identified here as a sister group to Suessiales but identified here as a sister group to Suessiales but

fig. S12, Supplementary Material online) in a common ancestor of all studied dinoflagellates [inferred by comparing the regressed ancestral sequence of all dinoflagellates studied to that of the regressed ancestral sequence of the common ancestor of all studied dinoflagellates and V. brassicaformis, which was the closest sister-group to dinoflagellates included in the alignment (Janouskovec et al. 2010)]. Comparing the two datasets, only four codons (ATA-Ile, AGA-Arg, ACC-Thr, and TAT-Tyr) were found both to occur at significantly higher frequencies in dinoflagellates than non-dinoflagellate species, and to have undergone a specific enrichment in the common ancestor of all studied dinoflagellates (supplementary table S5 and fig. S12, Supplementary Material online). Similarly, only one codon (CGT-Arg) was found to occur at a significantly lower frequency in dinoflagellates, and to have undergone a specific de-enrichment in the common ancestor of all studied dinoflagellates (supplementary table S5 and fig. S12, Supplementary Material online). Finally, only one amino acid (Tyrosine) was found to have undergone a significant change in frequency in the common ancestor of all studied dinoflagellates (supple mentary table S5 and fig. S12, Supplementary Material online), suggesting overall that relatively limited changes to plastid codon usage are associated with dinoflagellate origins.

Dinoflagellate-Wide Changes to Plastid Sequence Evolution

Elevated Pairwise Substitutions at the Origin of Dinoflagellates

Total numbers of pairwise substitutions were calculated for every species used in the multigene phylogeny, over the 4,478 nucleotide gap-free alignment (fig. 3; supplemen tary table S7, Supplementary Material online). The dinoflagellate sequences were highly divergent from the nondinoflagellate species (fig. 3; compare top left hand corner of figure to remainder). On average, dinoflagellate and

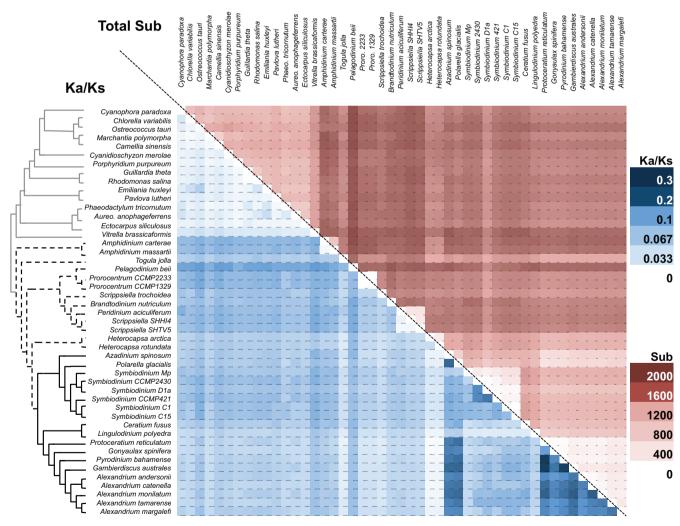


Fig. 3. Pairwise substitution ratios in peridinin dinoflagellates. This heatmap shows pairwise Ka/Ks ratios (bottom left hand sector) and total number of pairwise substitutions (top right hand sector) between every dinoflagellate and non-dinoflagellate sequence in the multigene nucleotide alignment. Sequences are shown per the multigene tree topology established in figure 2; non-dinoflagellates are shown on grey branches, basal dinoflagellates (Gymnodiniales, Peridiniales, Prorocentrales, and *Pelagodinium*) with dashed branches; and Gonyaulacales and Suessiales on solid black branches. The scale factors associated with each value are shown on the right-hand side of the figure. For ease of comparative viewing, the tree has been rooted here between the dinoflagellate and non-dinoflagellate lineages.

non-dinoflagellate species pairs were separated by 1,549 nucleotide substitutions, while pairs of non-dinoflagellate species were separated by an average of 994 substitutions, which was significantly lower (supplementary table S7 and fig. S14, panel A, Supplementary Material online; one-way ANOVA, $P = 1.86 \times 10^{-179}$). Even the related alveolate lineage *V. brassicaformis*, which was separated from other non-dinoflagellate species by a much larger number of substitutions (average value 1,276) was significantly less divergent than dinoflagellate species studied (supplementary table S7 and fig. S14, panel A, Supplementary Material online; $P = 1.2 \times 10^{-18}$), suggesting that this elevated substitution rate is specifically associated with dinoflagellate species.

We tested whether the elevated numbers of substitutions observed between dinoflagellate and non-dinoflagellate species were related either to plastid GC content, codon usage, or amino acid composition (supplementary figs. S14 and S15; supplementary results, Section 4, Supplementary Material online). While changes to plastid GC content and codon usage were correlated to the total numbers of pairwise substitutions observed (supplementary fig. S15, Supplementary Material online), alignment recoding to remove these effects did not eliminate the elevated substitution rates associated with dinoflagellate species (supplementary fig. S14, panel B, Supplementary Material online).

Elevated Ka/Ks Ratios at the Origin of Dinoflagellates

Pairwise Ka/Ks ratios (which provide information regarding the strength of selective pressure acting on individual sequences, as expressed by the ratio of non-synonymous to synonymous substitutions) were additionally calculated for each species pair (fig. 3; supplementary table S7, Supplementary Material online). Similar to the situation observed for total substitution rates, much higher pairwise Ka/ Ks ratios were observed between dinoflagellate and nondinoflagellate species pairs (average value 0.0592) than within non-dinoflagellate species pairs (supplementary fig. S16, panel A, Supplementary Material online; average value 0.0183; P = 2.75 \times 10⁻¹¹¹). A dramatic difference was also observed for the Ka/Ks ratios calculated between dinoflagellates and non-dinoflagellate species, and Vitrella and all other nondinoflagellate species (supplementary fig. S16, panel A, Supplementary Material online; average value 0.0271; P = 2. 87×10^{-18}).

We tested whether the elevated Ka/Ks ratios observed in dinoflagellates might be related to the extremely high total numbers of pairwise substitutions observed, for example due to a saturating substitution rate at codon third positions leading to an underestimate of the total synonymous substitutions between dinoflagellate and non-dinoflagellate species (supplementary figs. S17 and S18; supplementary results, Section 5, Supplementary Material online). The third position substitution rates between dinoflagellate and nondinoflagellate species, while high, were not at saturation rate (supplementary figs. S17 and S18; supplementary results, Section 5, Supplementary Material online). Other variables tested were either not correlated to the pairwise Ka/Ks ratios obtained (in the case of amino acid composition), or were not sufficient (judged by alignment recoding) to explain the differences in Ka/Ks ratios observed (in the case of third position GC content, and codon usage; supplementary figs. S16 and S19; supplementary results, Section 6, Supplementary Material online).

Lineage-Specific Changes to Peridinin Plastid Sequences

Extremely Elevated Ka/Ks Ratios within Dinoflagellates

Some dinoflagellate species were found to have extremely elevated pairwise Ka/Ks ratios calculated relative to other dinoflagellates in the alignment (fig. 3). For example, P. beii was separated from all other dinoflagellates by a minimum number of 1,400 substitutions, and Brandtodinium nutriculum was separated from all other dinoflagellates by a minimum number of 1,399 substitutions (fig. 3; supplementary table S7, Supplementary Material online), both of which were far larger than the average minimum number of total pairwise substitutions (416) calculated for other dinoflagellate species (Z-test, P < 0.05). These separations were found to be independent of plastid GC content and codon usage patterns in both species (supplementary fig. S20; supplementary results, Section 8, Supplementary Material online). Both species were also found to have elevated Ka/Ks ratios (minimum P. beii Ka/Ks 0.0618: minimum B. nutriculum Ka/Ks 0.0408: average dinoflagellate minimum Ka/Ks 0.0174; fig. 3), but these differences were eliminated by removing codon third positions from Ka/Ks calculations, suggesting that they are the result of saturating mutation rates in each species (supplementary fig. S20; supplementary results, Section 8, Supplementary Material online).

A dramatic evolutionary divergence was observed within members of the Gonyaulacales and Suessiales (fig. 3, bottom right hand sector; supplementary fig. S21, Supplementary Material online). Species within these lineages had extremely high pairwise Ka/Ks ratios, with a maximum value of 0.284 between the Gonyaulacales Protoceratium reticulatum and Pyrodinium bahamense, which is significantly greater than the average maximum pairwise Ka/Ks ratio (0.140) observed for all dinoflagellates (fig. 3; supplementary table S7, Supplementary Material online; Z-test, P < 0.05). The average pairwise Ka/Ks ratio between Gonyaulacalean and Suessialean dinoflagellates (0.110) was significantly higher than the average pairwise Ka/Ks ratio between other dinoflagellate pairs (0. 043; supplementary fig. S21, panel A, Supplementary Material online; $P = 1.57 \times 10^{-09}$). This was found to be independent of both third position substitutions, and changes to codon usage in these species (supplementary results, Section 8, Supplementary Material online). In contrast, the average number of pairwise substitutions between Gonyaulacalean and Suessialean species (711) was significantly lower (P = 0) than the average pairwise substitution frequencies observed between other dinoflagellates (1,417; fig. 3; supplementary fig. S21, panel B, Supplementary Material online), indicating that the rapid divergent evolution within this lineage is specifically due to an elevated Ka/Ks ratio.

Widespread Evolution of Alternative Translation Initiation Codons in Peridinin Plastids

44% of all the sequences identified lacked a plausible ATG initiation codon, hence probably use alternative translation initiation codons (supplementary table S8, Supplementary Material online). Eight different codons were identified as probable alternative initiation sites for individual peridinin

plastid transcripts, with TTG and ATT occurring the most frequently (fig.4; supplementary table S8, Supplementary Material online). None of the alternative translation initiation codons identified was conserved across all dinoflagellates, and the majority were species-specific (fig. 4, panel A). However, 20 alternative initiation codons were conserved across multiple dinoflagellate species (fig. 4, panel B, square labels), such

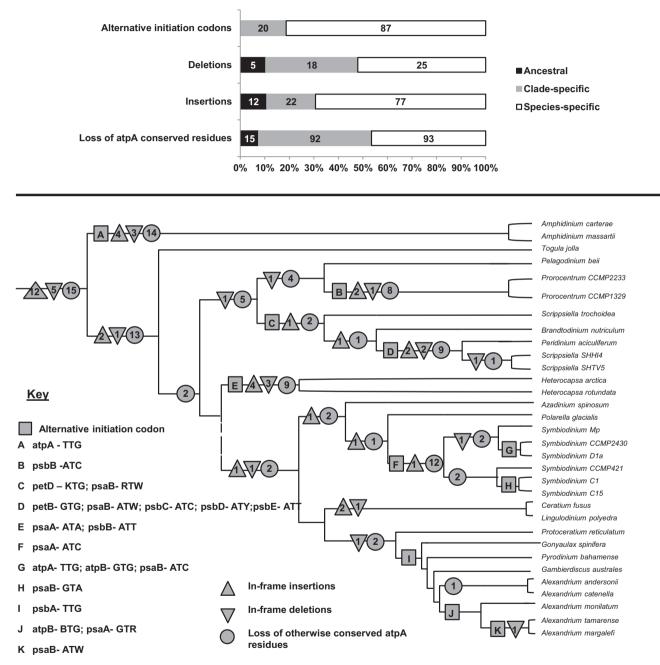


Fig. 4. Phylogenetic reconstruction of clade-specific evolutionary events in peridinin dinoflagellates. This figure shows discrete changes to peridinin plastid sequences that have occurred throughout dinoflagellate evolution. (A) shows the number of instances of four evolutionary events (adoption of alternative translation initiation codons, in-frame insertions and deletions, and the loss of otherwise conserved residues from atpA) that originated in a common ancestor of all dinoflagellates, are confined to specific species, or that originated in the common ancestors of specific dinoflagellate clades. (*B*) shows the phylogenetic origins of each of the clade-specific features, as determined by comparison to the multigene tree topology obtained in figure 2. Alternative initiation codons are shown with square labels, in-frame insertions and deletions with triangular labels, and discrete changes to otherwise conserved *atpA* residues with circular labels.

as the adoption of a TTG alternative initiation codon in *psbA* in a common ancestor of *Alexandrium*, *Gambierdiscus*, *Pyrodinium*, and *Gonyaulax* sp. (fig. 4, panel *B*, label *I*; supple mentary fig. S22, Supplementary Material online). Some lineages utilize alternative initiation codons more frequently than others, with six alternative initiation codons (petB-GTG, petD-KTG, psaB-ATW, psbC-ATC, psbD-ATY, psbE-ATT) found in *Scrippsiella hangoei* and its sister species *Peridinium aciculiferum* (fig. 4, panel *B*, labels *C*, *D*), compared with only one (atpA-TTG) in *Amphidinium* sp. (fig. 4, panel *B*, label *A*).

Multiple Discrete Changes to Plastid Protein Sequences within Dinoflagellates

A total of 111 insertions and 48 deletions distributed across 80 positions were identified within dinoflagellates (fig. 4, Panel A; supplementary table S9, Supplementary Material online). This contrasts to the situation for the non-dinoflagellate species in the alignment, for which only 19 insertions and 22 deletions were identified (supplementary table S9, Supplementary Material online). Twelve insertions and five deletions were conserved across all dinoflagellates (fig. 4, panel A; supplementary fig. S23, panel A, Supplementary Material online), although many of these indels have undergone substantial expansions or contractions in individual species (sup plementary fig. S23, panel B, Supplementary Material online). The majority of indels, however, were restricted to individual dinoflagellate species (77 insertions, 25 deletions) or clades (22 insertions, 18 deletions) (fig. 4, panel A; supplementary fig. S23, panel C, Supplementary Material online). These included two insertions (in PsaB, insertion starting at consensus residue 41; and PsbC, residue 197) and one deletion (in PsbB, starting at consensus residue 291) that evolved in a common ancestor of all species studied, except for the basally divergent Amphidinium, and one insertion (PsaB, residue 168) and one deletion (PsaB, residue 602) in a common ancestor of Gonyaulacales and Suessiales (fig. 4, panel B; triangular labels).

Instances in which a residue that is conserved in all other studied plastids was lost in dinoflagellates were tabulated for one representative protein, the ATP synthase subunit AtpA. 200 such changes were found, of which only 15 were ancestral (fig. 4, panel A; supplementary table S10, Supplementary Material online). Of the remaining 185 substitutions, 93 were species-specific, while 92 were shared across specific dinoflagellate clades. These clade-specific changes included the loss of 13 otherwise conserved residues in a common ancestor of Gonyaulacales and Suessiales (fig. 4, panel *B*, circular labels; supplementary table S10, Supplementary Material online).

Identification of Consistent Trends in Peridinin Plastid Evolution

Photosystem I Sequences in Peridinin Plastids Have Elevated Ka/Ks Ratios

An elevated dinoflagellate Ka/Ks ratio was observed in the two photosystem I subunit genes (*psaA* and *psaB*) retained in dinoflagellate plastids. For *psaA*, the dinoflagellate Ka/Ks ratio

(0.481) was 4.89 times that of the non-dinoflagellate value (0.098); whereas for *psaB* the dinoflagellate Ka/Ks ratio (0.446) was 4.47 times that of the non-dinoflagellate value (0.099; fig. 5, panel A). Both the Ka/Ks ratios observed were substantially greater than the average Ka/Ks ratios observed for all dinoflagellate plastid genes, both in terms of the raw Ka/Ks ratio (0.296) and in terms of the relative enrichment (2.41) compared with the non-dinoflagellate Ka/Ks ratios (0.123; fig. 5, panel A). Elevated Ka/Ks values were also obtained for dinoflagellate *psaA* and *psaB* genes in alignments recoded to eliminate third position substitutions and codon usage bias (supplementary fig. S24 and tables S11–S15; supplementary results, Section 8, Supplementary Material online).

Photosystem I Sequences in the Dinoflagellate Ancestor also Had Elevated Ka/Ks Ratios

Individual Ka/Ks ratios were also calculated for each gene, solely between the hypothetical sequences calculated for the common ancestor of all studied dinoflagellates, and the common ancestor of dinoflagellates and *Vitrella*, which should correspond to the substitutions that most probably occurred in the peridinin plastid immediately following its

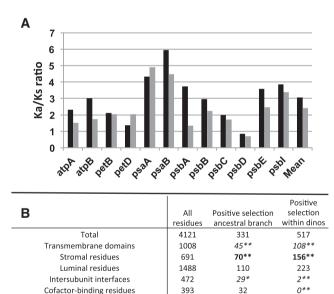


FIG. 5. Site-specific evolution in dinoflagellates. (A) shows the Ka/Ks residues calculated for each of the twelve peridinin plastid genes. Black bars show the Ka/Ks ratios inferred for the dinoflagellate common ancestor, divided by the Ka/Ks ratios calculated for every nondinoflagellate reference sequence within the alignments. Grey bars show the Ka/Ks ratios calculated within the dinoflagellate sequences, again divided by the Ka/Ks ratios calculated for the non-dinoflagellate sequences within the alignment. (B) tabulates the residues with adjusted Ka/Ks ratio >1, and Ka/Ks ratio significantly greater than corresponding non-dinoflagellate reference Ka/Ks ratio) in the common ancestor of all studied dinoflagellates or within the dinoflagellates (as above, except adjusted Ka/Ks ratio >0.5) and their predicted functional properties. Values that are significantly higher than would be expected through random distribution of these sites are shown in bold text, and values that are significantly lower are shown in italics. Values with one asterisk are significant to P < 0.05, and values with two asterisks are significant to $P < 1 \times 10^{-04}$.

divergence from other plastid lineages (supplementary table S11, Supplementary Material online). Elevated Ka/Ks ratios were found in both the dinoflagellate ancestor *psaA* (ancestral Ka/Ks 0.425; dinoflagellate ancestor/non-dinoflagellate ratio 4.32) and *psaB* sequences (ancestral Ka/Ks 0.593; dinoflagellate ancestor/non-dinoflagellate ratio 5.95), compared with all other genes (ancestral Ka/Ks 0.376; dinoflagellate ancestor/non-dinoflagellate ratio 3.07; fig. 5, panel A; supplementary tables S11 and S12, Supplementary Material online). The Ka/Ks ratios associated with the *psaB* dinoflagellate ancestor sequence were confirmed using alignment recoding to be genuine, rather than a consequence of a highly elevated mutation rate or change in codon usage preference specific to dinoflagellate photosystem I genes (supplementary Material online).

Elevated Ka/Ks Ratios Are Specific to Photosystem I Genes Only one other gene, psbl, was found to have a greater than average Ka/Ks ratio between dinoflagellates and nondinoflagellate species (dinoflagellate Ka/Ks 0.451; nondinoflagellate Ka/Ks 0.132; dinoflagellate/non-dinoflagellate ratio 3.39) and between the dinoflagellate ancestor and the common ancestor of dinoflagellates and Vitrella (dinoflagellate ancestor Ka/Ks 0.512; dinoflagellate ancestor/nondinoflagellate ratio 3.84; fig. 5, panel A; supplementary table S11, Supplementary Material online). However, the elevated psbl Ka/Ks ratio was eliminated in alignments recoded to eliminate third position substitutions (supplementary fig. S24; supplementary results, Section 8, Supplementary Material online), suggesting that it is the result is due to a saturating mutation rate at dinoflagellate psbl third codon positions. No other genes (except for psaA and psaB) were found to have elevated associated Ka/Ks ratios.

Stromal Domains of Peridinin Plastid Proteins Have Elevated Ka/Ks Ratios

Individual Ka/Ks ratios were calculated for each residue within each plastid gene, for dinoflagellates, non-dinoflagellate species, and the common ancestors of all studied dinoflagellates, and of all dinoflagellates and Vitrella (supplementary table S11, Supplementary Material online). The distribution of residues with elevated Ka/Ks ratios was biased toward specific regions of individual proteins. For example, within psbB, 59 codons have elevated associated Ka/ Ks ratios either in the common ancestor of all studied dinoflagellates (positions at the centre of a block of ten residues with aggregate Ka/Ks >1, and Ka/Ks significantly greater than that calculated for the equivalent non-dinoflagellate residue; Z-test, P < 0.05), or within the dinoflagellates (same criteria, but with Ka/Ks >0.5; supplementary fig. S25, Supplementary Material online). All of these codons are predicted to encode stromal- or luminal-facing residues (supple mentary fig. S25, Supplementary Material online).

Across the entire dataset, 171 of the 331 residues identified to have elevated Ka/Ks ratios in the common ancestor of all studied dinoflagellates were located on predicted stromal faces of plastid proteins (fig. 5, panel B; supplementary fig. S26, panel A, tables S11 and S12, Supplementary Material online). This is significantly greater than the number (123) expected through a random distribution of residues (chi-squared, $P = 6.43 \times 10^{-10}$; supplementary table S11, Supplementary Material online). The elevated Ka/Ks ratios on stromal residues were also identified in calculations performed with alignments recoded to eliminate third position substitutions and codon usage bias (supplementary fig. S26; supplementary results, Section 9, Supplementary Material online).

The same trends were not directly observed within individual dinoflagellate lineages, where the number of stromal residues with elevated Ka/Ks ratios was in fact slightly fewer than expected (202/582 residues; expected number 216; supple mentary fig. S26, panel B, and tables S11 and S12, Supplementary Material online). However, this may be influenced by the low Ka/Ks ratios observed in dinoflagellates for AtpA (0.251) and AtpB (0.254; fig. 5, panel A; supplementary table S11, Supplementary Material online), which are the only two proteins encoded in peridinin dinoflagellate plastids to be entirely extrinsic to the thylakoid membrane, hence entirely stromal-facing (Walker 2013). Excluding AtpA and AtpB, the number of residues with elevated Ka/Ks ratios in dinoflagellates that are predicted to face into the plastid stroma, was extremely greater than expected (172/552 residues with elevated Ka/Ks ratios; expected number of residues 29; P = 0; supplementary fig. S26, panel B; tables S11 and S12, Supplementary Material online). Similar to the dinoflagellate ancestor, the enrichment in dinoflagellate stromal Ka/Ks ratios was confirmed through alignment recoding to be genuine, rather than a result of mutation rate saturation or codon usage bias (supplementary results, Section 9, Supplementary Material online).

Discussion

We have identified and analyzed previously unannotated sequences for plastid-encoded transcripts in peridinin dinoflagellates. These data constitute over three times the number of previously annotated peridinin dinoflagellate plastid sequences, and increases the number of complete peridinin plastid protein-coding datasets 5-fold (fig. 1). Particularly large numbers of plastid transcript sequences were identified from the MMETSP transcriptome datasets (fig. 1). This may be due to the presence of the 3' poly(U) tail on dinoflagellate plastid transcripts, which has previously been speculated to enable the enrichment of plastid transcript sequences in poly(A) enriched RNA libraries (Wang and Morse 2006) such as those used for generation of the MMETSP transcriptomes (Keeling et al. 2014), and is corroborated by the presence of poly(U)tails on many of the transcripts we identified (supplementary fig. S1 and table S1, Supplementary Material online).

Almost all of the dinoflagellates investigated appear to possess the same 12 plastid-encoded protein-coding genes previously identified (Howe et al. 2008; Barbrook et al. 2014; Mungpakdee et al. 2014). We found no evidence for the relocation of any of these genes to the nucleus in any species (supplementary fig. S1 and table S1, Supplementary Material online) or the retention of other conventional plastid genes in any peridinin plastid (supplementary fig. S2 and table S2, Supplementary Material online). We additionally found only limited evidence for the presence of laterally acquired genes in the plastids of peridinin dinoflagellates, or that novel ORFs, previously identified in individual peridinin plastid lineages, may be conserved across multiple species (supplementary fig. S8 and table S2, Supplementary Material online). While we cannot formally exclude that other plastid transcripts [such as transcripts that do not receive a 3' poly(U) tail hence are unlikely to be present in poly(A)-enriched libraries] are produced, our data indicate that the 12 previously identified protein-coding genes represent the ancestral protein-coding component of dinoflagellate plastids.

These data have allowed us to produce a well-resolved reference tree for the branching relationships between major clades of peridinin dinoflagellates (fig. 2; supplementary figs. S9 and S10, Supplementary Material online). Several novel phylogenetic relationships were uncovered. For example, P. beii (previously Gymnodinium beii) grouped with the Prorocentrales with reasonable support (100/64%) whereas previous studies based on single-gene phylogenies placed it within the Suessiales (Siano et al. 2010; Decelle et al. 2014). Similarly, sister-group relationships between Prorocentrum and the Peridiniales, and the monophyletic clade of Gonyaulacales, Suessiales and Heterocapsa (fig. 2), have not to our knowledge been previously described (Hoppenrath and Leander 2010; Bachvaroff et al. 2014; Gavelis et al. 2015). Each of these novel relationships were also recovered using modified alignments from which long branches, individual genes, gapped positions, or fast-evolving sites were removed (supplementary figs. S9 and S10, Supplementary Material online). We accordingly conclude that the relationships obtained within our dataset are probably genuine, and not the artifact of fast sequence evolution or recent discrete changes (such as changes to plastid translation tables, which might bias the conceptual translations obtained, but presumably should be removed in the fast site analysis) in individual dinoflagellate plastids.

We have correlated divergent changes to peridinin plastid transcript sequences to the branching relationships from the multigene phylogeny, allowing us to infer when these changes occurred. For these analyses, we have focused exclusively on the sequences and conceptual translations of plastid transcripts, which provide an understanding of the aggregate consequences of divergent gene evolution and transcript editing on peridinin plastids (Zauner et al. 2004; Bachvaroff et al. 2006; Dorrell and Howe 2015). As many of the sequences identified from MMETSP possess poly(U) tails (supplemen tary fig. S1 and table S1, Supplementary Material online), and the presence of the poly(U) tail is associated with the completion of transcript editing in dinoflagellate plastids (Dang and Green 2009; Dorrell et al. 2016), we presume that the majority of the sequences identified in this study probably have been edited to completion, as opposed to representing unedited precursor transcripts.

First, we have identified changes to peridinin plastid sequence composition across the dinoflagellates. These include changes to plastid sequence GC content and codon usage (supplementary figs. S11 and S12, Supplementary Material online), although many of these changes are either shared with relatives (such as the elevated third position GC content in the chromerid Vitrella; supplementary fig. S11, Supplementary Material online), or appear largely to consist of changes specific to individual dinoflagellate lineages (such as the changes to plastid codon usage frequencies, which are much more numerous in extant dinoflagellate species than in the inferred sequences of their last common ancestor; supple mentary fig. S12, Supplementary Material online). We could not find convincing evidence for changes to the plastid translation table across the dinoflagellates (supplementary fig. S13, Supplementary Material online). While we cannot exclude alternative hypotheses (e.g., independent increases in third position GC content in the lineages giving rise to Vitrella, and in a common ancestor of all dinoflagellates), we cannot find sufficient evidence for major changes to plastid sequence composition, or translation, occurring in the dinoflagellate common ancestor.

Next, we have identified widespread changes to the translation products of plastid sequences in dinoflagellates. These include changes resulting from large numbers of substitutions, and greatly elevated Ka/Ks ratios associated with dinoflagellate plastid transcripts (fig. 3; supplementary figs. S14 and S16, Supplementary Material online). The elevated Ka/Ks ratios are unlikely to be explained by changes in codon preference (supplementary figs. S11 and S16, Supplementary Material online), or saturation of synonymous substitution rates at third-position sites in dinoflagellate plastids (supple mentary figs. S17-S19, Supplementary Material online). It is possible that other factors related to sequence composition (e.g., transitory changes in codon preference in individual dinoflagellate lineages, or saturation of synonymous substitution rates at first- and second-position sites) may have contributed to the elevated Ka/Ks ratios observed; however, we suggest that the most parsimonious explanation for the remaining elevated Ka/Ks ratios observed in dinoflagellate plastids are changes in plastid selection pressure throughout their evolution, commencing after their divergence from other plastid lineages, and throughout the radiation of extant species. Although previous studies have posited changes in selection pressure on certain peridinin plastid genes (Shalchian-Tabrizi et al. 2006), this is to our knowledge the first evidence that indicates that selective events have played a widespread role in dinoflagellate plastid evolution.

We have additionally identified changes that have occurred in individual dinoflagellate lineages since their radiation (figs. 3 and 4; supplementary figs. S20–S23, Supplementary Material online). We have found extremely elevated Ka/Ks ratios in pairwise comparisons between dinoflagellates (fig. 3; supplementary figs. S20 and S21, Supplementary Material online), and map multiple acquisitions of alternative translation initiation codons (supplemen tary fig. S22, Supplementary Material online), in-frame insertion and deletions (supplementary fig. S23, Supplementary Material online), and the loss of otherwise conserved *atpA* residues to the dinoflagellate tree (fig. 4). These events have occurred progressively, with the majority of the dinoflagellate clades being marked by discrete changes to plastid sequences (fig. 4), and contrasts with the much more conservative evolution observed in other plastid lineages (supplementary ta bles S8 and S9, Supplementary Material online). The divergent evolutionary events observed in this study await detailed biochemical characterization. For example, it will be interesting to determine experimentally whether peridinin dinoflagellates utilize the alternative translation initiation codons identified in this study, or whether there are further translation initiation codons with weaker similarity to ATG in peridinin plastids. This could be accomplished, for example, by proteomic characterization of the N-termini of peridinin plastid proteins (Huesgen et al. 2013). Regardless, our data show that peridinin plastid sequences have not remained static, but have continued to diverge from one another to a remarkable extent.

We have found evidence that different peridinin plastid lineages have evolved in different manners since their radiation. For example, we observe elevated minimum pairwise substitution rates in some Peridinialean/Prorocentralean species (e.g., Brandtodinium, Pelagodinium; fig. 3), which is corroborated by the rather long branch lengths associated with these species in the multigene tree (fig. 2; supplementary fig. S9, Supplementary Material online), and appears to explain at least partially the high Ka/Ks ratios observed for these species (supplementary fig. S20, Supplementary Material online). We also observe extremely high maximum pairwise Ka/Ks ratios within members of the Gonyaulacales and Suessiales, but in contrast these occur alongside relatively low pairwise substitution rates, suggesting that they have resulted from a change in plastid selective pressure in these lineages (fig. 3; supple mentary fig. S21, Supplementary Material online). Similarly, we have found that specific nodes on the peridinin plastid tree are marked by the origins of large numbers of alternative initiation codons (the common ancestor of S. hangoei and P. aciculiferum; fig. 4), indels (the common ancestor of Amphidinium and Heterocapsa; fig. 4), or changes to conserved *atpA* residues (the common ancestor of Symbiodinium; fig. 4). It remains to be determined why the plastids of specific dinoflagellate lineages and not others are unusual, although we note that many of the most divergent species within our dataset have symbiotic life strategies (e.g., Pelagodinium is an endobiont of foraminiferans; Siano et al. 2010, whereas Brandtodinium is a radiolarian symbiont; Probert et al. 2014). More taxonomically detailed comparisons of plastid evolution in endosymbiotic dinoflagellates to their free-living relatives may provide insights into whether symbiosis has driven divergent plastid evolution within the dinoflagellates.

More globally, it remains to be resolved why the peridinin dinoflagellates have undergone such divergent plastid evolution compared with other lineages. Notably, we show that residues with elevated Ka/Ks ratios in peridinin plastids are concentrated, both in extant dinoflagellates and in the dinoflagellate common ancestor, on photosystem I subunits, and stromal regions of plastid proteins, which cannot be explained by changes to codon usage or third position substitution rate (fig. 5; supplementary figs. S24–S26, Supplementary Material online). While divergent evolution has previously been reported in the photosystem I sequences in individual peridinin plastid lineages (Bachvaroff et al. 2006; Shalchian-Tabrizi et al. 2006; Pochon et al. 2014), this is to our knowledge the first evidence that this bias in evolutionary events is conserved throughout peridinin plastids, from the origin of dinoflagellates to extant species.

Similar, albeit less extreme divergent evolution events to those described in this study have been observed in nuclear genes encoding plastid-targeted proteins (Bachvaroff et al. 2006; Mungpakdee et al. 2014) and non-plastid proteins (Kim et al. 2011) in peridinin dinoflagellates. It will be interesting to determine if the divergent evolutionary events observed in nucleus-encoded and plastid-encoded genes are linked; for example if the nucleus-encoded components of dinoflagellate photosystem I, or nucleus-encoded proteins likely to interact with the stromal faces of plastid-encoded dinoflagellate proteins, likewise possess specifically elevated Ka/Ks ratios. Conserved trends in the evolution of nucleus and plastid-encoded proteins in dinoflagellates might arise as a result of compensatory evolution events to maintain plastid physiology (e.g., maintaining plastid redox state for plastid physiology and gene regulation (Allen 1993; Puthiyaveetil et al. 2008), or balancing cyclic and linear electron flow to meet the physiological requirements of individual lineages (Reynolds et al. 2008)), or as a result of divergent selection on plastid proteins to accommodate some of the more unusual nucleus-encoded proteins and structures present in peridinin plastids, (e.g., the dinoflagellate pyrenoid (Nassoury et al. 2005; Siano et al. 2010), or the peridinin pigment-binding protein complexes (Haxo et al. 1976)). Ultimately, understanding the relationships between peridinin plastid sequences, evolution and physiology may provide valuable insights into the biology of this unusual and ecologically important lineage.

Materials and Methods

Assembly and Annotation of Previously Known Peridinin Plastid Sequences

Nucleotide sequences corresponding to the 12 protein-coding genes (atpA, atpB, petB, petD, psaA, psaB, psbA, psbB, psbC, psbD, psbE, psbI) that are found on the three effectively complete peridinin plastid genomes (A. carterae CCAP1102/ 6; Symbiodinium sp., Clade C3, and Clade Mf) (Nisbet et al. 2004; Barbrook et al. 2014; Mungpakdee et al. 2014), were assembled from peridinin dinoflagellate EST libraries within NCBI (https://www.ncbi.nlm.nih.gov/, last accessed June 16, 2014) and the Marine Microeukaryote Transcriptome Sequencing Project (MMETSP) (http://data.imicrobe.us/proj ect/view/104, last accessed November 1, 2014) (Keeling et al. 2014). Sequences were identified by tBLASTn searches, using annotated plastid protein sequences from peridinin dinoflagellates and their close relatives (listed in supplementary table S1, Supplementary Material online). Where possible, the predicted translation products of plastid transcript sequences were used, instead of the translation products of plastid gDNA sequences, due to the presence of plastid transcript editing in some dinoflagellates (Zauner et al. 2004; Dorrell and Howe 2015).

Sequences that matched the queries with expect values of below 1×10^{-5} were selected, and were searched using BLASTx against the entire NCBI database. Sequences that yielded a top hit against another peridinin dinoflagellate sequence were retained for subsequent analysis. Sequences that were excluded on the basis of being of probable non-dinoflagellate origin are listed in supplementary table S1, Supplementary Material online. In the case of *psbl*, for which peridinin dinoflagellate sequences are known to be highly divergent (Nisbet et al. 2004), an initial expect value threshold <1.0 was used to identify possible dinoflagellate orthologues, and these orthologues were used in turn as query sequences for a second round of reciprocal tBLASTn/BLASTx searches against each dataset, to identify even the most divergent sequences present.

To investigate whether novel plastid ORFs, and genes proposed to have been acquired by lateral transfer from Bacteroidetes are conserved across peridinin plastids, similar BLAST searches were performed with the translation products of the four predicted ORFs (*ORF1, ORF2, ORF3,* and *ORF4*) described in the *A. carterae* plastid genome (Barbrook et al. 2001; Nisbet et al. 2004; Barbrook et al. 2006), and the proposed *ycf24* and *ycf16* genes from *C. horridum* (Moszczynski et al. 2012). For these genes, sequences were retained if the top reciprocal BLAST hit was homologous to the genes in question, regardless of evolutionary affinity.

Sequences that passed the reciprocal BLASTx search were assembled into contigs using GenelOUS v 4.76 (Kearse et al. 2012). Each nucleotide sequence was searched manually for possible 5' spliced leader sequences (Zhang et al. 2007), and uninterrupted 3' poly(T) and poly(A) tracts of more than 3bp length, which might respectively correspond to transcript poly(U) and poly(A) tails (Wang and Morse 2006). The predicted translation products of each contig were inspected for the presence of possible plastid-targeting sequences using SignalP version 3.0 (Bendtsen et al. 2004) and ASAFind (Gruber et al. 2015), and for mitochondria-targeting sequences using TargetP version 1.1 (Emanuelsson et al. 2007) under the default conditions. Annotated copies of each novel peridinin plastid transcript (including information on the presence of possible poly(U) tails, poly(A) tails, spliced-leader sequences, and plastid-targeting sequences) are included in supplemen tary table S1, Supplementary Material online.

Global Identification and Annotation of Peridinin Plastid Transcripts

To determine whether further, previously undocumented ORFs are conserved across peridinin plastids, an independent, top-down search was performed for the entire dinoflagellate sequence library. We focused on transcripts possessing a 3' poly(U) tail, as this feature is believed to be uniquely associated with plastid transcripts in dinoflagellates (Dorrell and Howe 2012), and polyuridylylated transcripts have previously been indicated to be enriched by poly(A) selection, hence may be present in poly(A)-selected transcriptome datasets such as MMETSP (Wang and Morse 2006; Keeling et al. 2014).

For this analysis, all sequences that terminated at either end in a potential poly(T) sequence (>3 bp) from all RNA libraries were extracted, and filtered to remove sequences that either contained a more plausible reverse complement of a poly(A) sequence (length of poly(A) sequence \geq poly(T) sequence), or a spliced-leader (\geq 6-bp spliced-leader sequence) on the other transcript end. Parallel libraries were constructed, containing all dinoflagellate sequences that by the same criteria possessed either a poly(A) tail, or spliced-leader sequences were searched against these libraries using tBLASTx. Poly(T)-containing sequences that were contiguous with other poly(A) or spliced-leader containing sequences (as judged by BLAST best hit; expect value <1 × 10⁻⁵, >90% similarities) were likewise removed from the dataset.

Next, to identify sequences encoding proteins of probable plastid function, the filtered poly(T)-containing sequences were oriented such that the poly(T) sequence was located on the transcript 3' end, and searched by BLASTx against a composite protein dataset, consisting of the complete protein sequences encoded in the nuclear and plastid genomes of the model diatom Phaeodactylum tricornutum (Oudot-Le Secq et al. 2007; Bowler et al. 2008) (http://protists.ensembl. org/Phaeodactylum tricornutum/Info/Index, last accessed March 14, 2015), and all dinoflagellate plastid sequences previously identified by the BLAST searches detailed above. Sequences that yielded a top hit in a reverse orientation reading frame (i.e., such that the poly(T) sequence could not be located on a transcript 3' end), or were identified to correspond to an internal region of a transcript (judged if the 3'end of the transcript alignment corresponded to <90% the full length of the subject length), that yielded a top hit against a known dinoflagellate plastid protein, or that yielded a top hit against a Phaeodactylum nucleus-encoded protein (expect value $< 1 \times 10^{-5}$) were removed.

The longest ORFs from sequences that were found to possess plausible 3' ends, and were homologous to plastid-encoded proteins in Phaeodactylum that have not previously been identified in peridinin dinoflagellate plastids were extracted, and searched for the presence of plastid- and mitochondria-targeting sequences as above. The sequences for which no plausible BLAST hit was found (and thus may contain novel plastid ORFs), were searched against one another using reciprocal tBLASTx/ tBLASTx searches. Sequences that were found to match one another with a reciprocal BLAST hit expect value of $< 1 \times 10^{-5}$ (and thus might correspond to conserved novel plastid proteins) were retained, assembled into contigs, and aligned using GeneIOUS v 4.76, as above. The final annotations for each poly(T)-containing sequence, as well as full nucleotide and protein sequences for the possible novel plastid ORFs identified, are presented in supplementary table S2, Supplementary Material online.

Phylogenetic Analysis

To assess the phylogenetic relationships between the different dinoflagellates studied, conceptual translations were generated for each novel peridinin plastid sequence identified from the MMETSP libraries (Keeling et al. 2014), using a standard translation table. This and all subsequent analyses conducted throughout the remainder of the study were restricted to proteins generated through the conceptual translations of plastid transcript sequences, to minimize complications resulting from the comparison of (edited) transcript sequences and (unedited) gene sequences, and to reflect the probable eventual translation products of each plastid sequence.

The conceptual dinoflagellate protein sequences for each gene were aligned, using 20 iterations of MUSCLE v 3.8 (Edgar 2004), to a reference set of orthologous sequences from 15 other plastid lineages, including a chromerid (V. brassicaformis) that represents the closest documented plastid-containing relative of the peridinin dinoflagellates (Janouskovec et al. 2010). Orthologues from other alveolate plastids (those of apicomplexans, and the chromerid Chromera velia) were not included, due to the loss of photosynthesis genes (in the case of apicomplexans), or the exceptionally divergent nature of the plastid genome, including changes in the plastid translation table (in the case of C. velia) (Moore et al. 2008; Janouskovec et al. 2013). The petD sequence from Ostreococcus tauri was excluded from this and all subsequent analyses, as it is not present within the O. tauri plastid genome (Derelle et al. 2006; Robbens et al. 2007).

The alignments were manually corrected, trimmed to remove all positions at which the most common nonambiguous identity was a gapped position, and concatenated. For single-gene trees of *rpl28, rpl33, ycf16* and *ycf24* sequences, similar alignments were generated, in this case containing all of the novel sequences identified, the previously annotated *P. lunula* and *C. horridum* sequences (Moszczynski et al. 2012), and a representative sample of sequences from different plastid and bacterial lineages, and trimmed as before. All of the multiple- and single-gene alignments generated for inference of phylogenetic trees are provided in supplementary table S3, Supplementary Material online.

Bayesian inference of single gene alignments was carried out using PhyloBayes v3.3 (Lartillot et al. 2009), with default settings and the LG $+ \Gamma$ model. Two chains were run in parallel, using the automatic stopping rule such that sampling was conducted every 100 points until the maximum difference was \leq 0.1 and the effective size \geq 100. Bayesian analyses of concatenated alignments were performed using MrBayes 3.2.6 hosted on the CIPRES Science Gateway webportal (Ronquist et al. 2012; Miller et al. 2015). For each dataset, two independent runs were performed, each comprising four chains for 1,000,000 MCMC generations, sampling every 1,000 points and selecting the first quarter as burn-in for the consensus. The burn-in was selected such that the resulting standard deviation of split frequencies was <0.06 for all datasets, and that the log likelihood of the cold chain had reached a stable plateau. Analyses were run with model mixing and Γ distributed rate categories with an additional invariant category.

All Maximum Likelihood analyses were carried out using RAxML v8.1.17 (Stamatakis 2014), under the LG + Γ model, as hosted on CIPRES (https://www.phylo.org/, last accessed March 26, 2016). For analyses of both Bayesian and Maximum Likelihood inference, the -b option was used to conduct 500

non-parametric bootstraps. These were then subsequently assembled into a consensus tree using the consense program of the PHYLIP package (v3.695) on default settings. Bipartitions present in both trees were mapped onto the Bayesian topology. Trees based solely on Maximum Likelihood were run using the -f option, such that bootstraps were automatically mapped onto the Maximum Likelihood estimate of the tree from the same run. In all cases, gamma distributed rates were modeled under a discrete model with four rate categories. Newick format tree outputs for each alignment, under each condition tested, are provided in sup plementary table S4, Supplementary Material online.

Alignments from which individual genes or all gapped positions were removed were constructed using GeneIOUS. Ten further alignments were constructed from which the species corresponding to the ten longest branches obtained in the initial Bayesian consensus tree analysis were serially removed. Finally, the evolutionary rate associated with each position within the alignment was calculated using TIGER, with the -b 100 option (Cummins and McInerney 2011). Fifteen alignments were constructed, from which the 25 fastest evolving categories were serially removed. All modified alignments were tested using RAx/ML using the same conditions as previously defined. Modified alignments and TIGER output data for fast site identification are supplied in supplementary table S3, Supplementary Material online.

Codon Usage Comparisons

Changes in nucleotide sequence composition across the peridinin dinoflagellates were assessed over the six genes (psaA, psaB, psbA, psbB, psbC, and psbD) for which sequences had been identified in each dinoflagellate MMETSP library studied. Due to the probable sequence contamination present, the Symbiodinium Clade A library was excluded from this and all subsequent analyses (fig. 2). First, nucleotide alignments of each gene were generated, and manually trimmed to remove insertions specific to dinoflagellate lineages; these alignments were concatenated to produce an alignment of all six genes (supplementary table S3, Supplementary Material online). GC content and codon usage frequencies of each sequence within the alignment were calculated using PAML v4.8 (Yang 2007), using a standard genetic code. Amino acid composition of each species was quantified by summing the different codon frequencies obtained. To assess the relative codon usage frequencies, and amino acid composition biases associated with each species, the average frequency of each codon, and each amino acid, were calculated for all species in the alignment. The sum of squares of difference between the frequencies of each codon, or amino acid for each species, and the alignment-wide mean values, were calculated, and then ranked in ascending order. All statistics pertaining to codon and amino acid frequency are provided in supplementary table S5, Supplementary Material online.

To assess the distribution and form of translationally invariant sites in dinoflagellate plastids, untrimmed nucleotide alignments were generated for each gene. dN and dS ratios were calculated for each site, within each gene, for dinoflagellate sequences only, using PAML v4.8 under a standard genetic code. All codon positions within each alignment with an observed Ka of 0 (i.e., no non-synonymous substitutions) within the dinoflagellates were extracted, and are shown in supplementary table S6, Supplementary Material online.

Finally, to assess which of the trends identified might represent ancestral changes to dinoflagellate plastid translation, predicted ancestral sequences of each plastid sequence were generated by regression using PAML as before (supplemen tary table S3, Supplementary Material online). Two sequences were generated, one corresponding to the common ancestor of all studied dinoflagellates included in this study, and one corresponding to the common ancestor of dinoflagellates and *V. brassicaformis*, the closest sister-group to dinoflagellates within the alignment. Codon frequencies associated with each ancestral sequence were calculated using PAML v4.8 as before, and compared with one another.

Nucleotide Sequence Substitutions

Pairwise Ka/Ks ratios and total numbers of pairwise substitutions were calculated using the gap-free concatenated nucleotide alignment, for each possible combination of species, with KaKs Calculator version 2.0, using the Model Averaging method (which performs weighted calculations using eight different substitution matrices, based on the relative likelihood of each matrix to explain the observed sequences) and a standard plastid genetic code (Wang et al. 2010). Pairwise Ka/Ks calculations and the total number of substitutions for each species pair are provided in supplemen tary table S7, Supplementary Material online.

To investigate the different factors underpinning substitution rates within the alignment, total numbers of pairwise substitutions and Ka/Ks ratios were correlated against (1) the third-position GC content, (2) the codon usage bias (defined as above), and (3) the amino acid composition bias for each species pair. Correlation calculations were performed for both the average values and modular differences in each variable for each species pair, and were performed for both the absolute substitution rates and Ka/Ks ratios observed, and the rank of each value within the entire dataset. Third-position GC, amino acid composition bias and codon usage bias values for each species are provided in supplementary table S5, Supplementary Material online, and values for each species pair are provided in supplementary table S7, Supplementary Material online.

Mutation rate saturation was assessed using the DAMBE software package (Xia et al. 2003). The concatenated gap-free alignment was separated into first-, second-, and third-codon positions only, and separate calculations were performed for each codon position. A separate series of calculations were additionally performed for each codon position using alignments consisting only of the dinoflagellate sequences from the first-, second-, or third-position alignments. For each alignment and codon position, the proportion of invariant sites was first calculated, using the tree topology obtained using the multigene phylogeny (supplementary table S4, Supplementary Material online), under otherwise default conditions. Substitution rates were then assessed at each co-don position through each alignment using Xia's test, with

the empirically verified invariant site frequencies (Xia et al. 2003; Xia 2013), and otherwise under the default conditions.

To determine whether any of the above factors have had significant effects on the total numbers of pairwise substitutions observed, the total number of pairwise substitutions and Ka/Ks ratios were calculated for alignments that were manually recoded in several ways (all modified alignments provided in Supplementary table S3, Supplementary Material online). To investigate the affect of GC content shifting on substitution rates, total numbers of pairwise substitutions were calculated for alignments that had been RYrecoded (Ishikawa et al. 2012). Two RY-recoded alignments were produced: one alignment in which all adenosines were replaced by guanosines and all thymidines were replaced by cytosines, and one for which the converse substitutions were performed. To investigate the different roles of each codon positions on substitution rates, total numbers of pairwise substitutions were calculated for the separate first, second and third position alignments previously generated for inspection with DAMBE, and two further alignments consisting only of third codon positions that had been manually RYrecoded as above (supplementary table S3, Supplementary Material online). To investigate the significance of third position mutations on Ka/Ks, ratios were calculated for two alignments that had been manually recoded so that all third codon positions were replaced either by adenosines, or by guanosines (supplementary table S3, Supplementary Material online). These two substitutions were performed as they preserve the possibility for synonymous first-position substitutions associated with leucine (YTR) and arginine codons (RGR), whereas manual recoding of the third position to pyrimidine nucleotides would eliminate all synonymous single substitutions associated with 6-fold degenerate codons under a standard genetic code (Crick 1968; Inagaki et al. 2004). Finally, to investigate the effects of changes in dinoflagellate plastid codon preference on Ka/Ks and substitution rates, calculations were performed for an alignment which was globally recoded so that 19 codons, which occur at significantly lower frequencies in dinoflagellates than in non-dinoflagellate species (one-way ANOVA, P < 0.05), were universally replaced with 19 synonymous codons that occur at elevated frequencies in dinoflagellates (supplementary ta ble S5, Supplementary Material online). Pairwise substitution value calculations for all manually recoded alignments are provided in supplementary table S7, Supplementary Material online.

Translation Initiation Site Identification

Possible alternative translation initiation codons in peridinin plastids were identified from nucleotide sequence alignments of each sequence that contained all of the dinoflagellate sequences studied, and orthologues from each of the nondinoflagellate reference sequences used for construction of the multigene phylogeny. The 5' end of each nucleotide sequence was trimmed so that it started from the first in-frame termination codon within the 5' UTR, or (if no such codon existed) so that the coding sequence was located within reading frame position +1.

To determine which alternative translation initiation codons are utilized in peridinin plastids, the most probable initiation codon was identified in the N-terminal coding region of each dinoflagellate sequence using a custom-built automated pipeline (supplementary text S1, Supplementary Material online). As the presence of Shine-Dalgarno sequences in peridinin plastid genomes remains unclear (Zhang et al. 1999; Dang and Green 2009), initiation codons were searched for in the entire possible 5' coding region of each sequence. This was defined as the region extending upstream from the first residue that was identical in 75% of the nondinoflagellate reference sequences. The most probable initiation codon was taken to be ATG, if such a codon were present. If not, the sequence was screened for codons that shared two bases in common with ATG, which has been shown experimentally in other plastid lineages to be sufficient to permit translation initiation (Chen et al. 1995), alongside GTA, which has been documented to function as an alternative initiation codon in Proteobacteria (Kim et al. 2008), and has previously been proposed to be used as an alternative translation initiation codon in Amphidinium (Barbrook and Howe 2000; Barbrook et al. 2001). The nearest codon to the consensus initiation site in the non-dinoflagellate reference species (hence would produce the ORF with the greatest homology to the expected protein sequence) was then taken as the most probable translation initiation site. These data, including full lists of all codons deemed to be possible initiation codons for each gene and in each species, as well as the most probable initiation codons, are provided in supplemen tary table S8, Supplementary Material online.

Indel Analysis

Indels within peridinin plastid sequences were identified using untrimmed protein sequence alignments generated for each gene, as above. Pairwise comparisons were performed between each dinoflagellate sequence and non-dinoflagellate sequence previously used for the construction of the multigene alignment, using a custom built Python script that automatically detects and reports both insertions and deletions (supplementary text S2, Supplementary Material online). Sequences were counted as insertions only if they occurred in at least one dinoflagellate sequence but were absent from all of the non-dinoflagellate reference sequences, or as deletions if they were absent from at least one dinoflagellate but were present in every reference sequence examined.

Each predicted indel was confirmed by visual inspection of the alignment. Positions that were within five amino acids of sequence N- or C-termini, and patterns of alternating insertions and deletions that indicated poor alignment of the sequence were rejected. Tabulated indels identified for each species, and the inferred phylogenetic origin point (as defined using the multigene tree topology) of each indel is shown in supplementary table S9, Supplementary Material online.

Changes to Conserved atpA Residues

Changes to residues that were conserved in all other plastid lineages were identified by visual inspection of the untrimmed atpA protein sequence alignment containing all of the dinoflagellate sequences studied, each of the nondinoflagellate reference sequences used for generation of the multigene phylogeny. Residues were deemed to be conserved in non-dinoflagellate lineages only if they were found in all, or all but one, of the species studied, including the closest relative to the dinoflagellates within the alignment (*V. brassicaformis*). The full list of substitutions to conserved AtpA residues for each species, alongside the inferred origin points for each substitution, is provided in supplementary table S10, Supplementary Material online.

Site-Specific Substitution Rates

Substitution rates for each residue within each sequence were calculated using the previously constructed single-gene nucleotide alignments. Each sequence was trimmed to remove indels that were specific to dinoflagellates, and Ka/Ks ratios were calculated for each site using PAML v 4.8, site model constraint 2, and a standard plastid genetic code (Yang 2007). The consensus multigene tree generated above was used as the reference tree topology. Separate alignments were constructed for each sequence in which the codon third positions were either manually recoded to adenosines or to guanosines, or in which all codon positions were manually altered to reflect the predominant codon usage patterns observed in dinoflagellates, as detailed above. Raw and modified alignments for each sequence are provided in supplementary table S3, Supplementary Material online, and the Newick format trees used for each analysis in supplementary table S4, Supplementary Material online.

To allow comparisons between the evolutionary rates observed for dinoflagellate and non-dinoflagellate species, separate values were calculated for each site, using only dinoflagellate sequences, and using only non-dinoflagellate sequences. To identify substitution events that occurred at the divergence of peridinin dinoflagellates from other plastids, values were also calculated for each gene for the previously inferred sequence for the dinoflagellate common ancestor, when compared directly to the sequence for the common ancestor of dinoflagellates and *Vitrella* (supplementary table S3, Supplementary Material online). Individual rate calculations for each gene, including gene length, are provided in supplementary table S11, Supplementary Material online.

Averaged Ka/Ks ratios were then calculated over a sliding window of eleven residues in each sequence. For regions of sequence which through this approach contained no synonymous substitutions, the sliding window was expanded to include the nearest codon upstream, and the nearest codon downstream that were found to have undergone synonymous substitutions. The residues with Ka/Ks ratios >1 in the dinoflagellate common ancestor, or Ka/Ks ratios >0.5 within dinoflagellates were inspected for localization (transmembrane, stromal, or luminal-facing), and function (interaction with other plastid-encoded subunits, or with nucleusencoded subunits and cofactors), as inferred by alignment to annotated PDB sequences from the plastid of Arabidopsis thaliana (Sato et al. 1999), and the model cyanobacterium Thermosynechococcus elongatus (Kamiya and Shen 2003). Separate Ka/Ks calculations were also performed and annotated for the previously generated codon re-optimized, third-position adenosine- and third-position guanosine recoded alignments (supplementary table S3, Supplementary Material online), with substitution values for each alignment provided in supplementary tables S12– S15, Supplementary Material online.

Data Deposition

All sequences and supplementary tables referenced in this study are publically accessible from the University of Cambridge dserve server (https://www.repository.cam.ac.uk/handle/1810/252774; last accessed November 8, 2016).

Supplementary Material

Supplementary data are available at *Molecular Biology and Evolution* online.

Acknowledgments

This study was supported by a Research in Paris post-doctoral fellowship [to RGD] from the Mairie de Paris (grant number 2014/89), a Canada Vanier Graduate Scholarship and an Alberta Innovates Health Solutions Graduate Studentship [both to CMK], an AITF grant award [to ER] and a Wellcome Trust project grant (grant number 094249) to [CJH and RERN]. Work in the Bowler lab is supported by the ERC Advanced Award Diatomite and the LouisD Foundation of the Institut de France. Work in the Dacks lab is supported by a Discovery Grant from the Natural Sciences and Engineering Research Council of Canada (RES 0021028). JBD is the Canada Research Chair in Evolutionary Cell Biology.

References

- Allen JF. 1993. Control of gene expression by redox potential and the requirement for chloroplast and mitochondrial genomes. *J Theor Biol.* 165:609–631.
- Bachvaroff TR, Concepcion GT, Rogers CR, Herman EM, Delwiche CF. 2004. Dinoflagellate expressed sequence tag data indicate massive transfer to the nuclear genome sequence. *Protist* 155:65–78.
- Bachvaroff TR, Gornik SG, Concepcion GT, Waller RF, Mendez GS, Lippmeier JC, Delwiche CF. 2014. Dinoflagellate phylogeny revisited: using ribosomal proteins to resolve deep branching dinoflagellate clades. *Mol Phyl Evol.* 70:314–322.
- Bachvaroff TR, Sanchez-Puerta MV, Delwiche CF. 2006. Rate variation as a function of gene origin in plastid-derived genes of peridinincontaining dinoflagellates. J Mol Evol. 62:42–52.
- Barbrook AC, Dorrell RG, Burrows J, Plenderleith LJ, Nisbet RER, Howe CJ. 2012. Polyuridylylation and processing of transcripts from multiple gene minicircles in chloroplasts of the dinoflagellate Amphidinium carterae. Plant Mol Biol. 79:347–357.
- Barbrook AC, Howe CJ. 2000. Minicircular plastid DNA in the dinoflagellate Amphidinium operculatum. Mol Gen Genet. 263:152–158.
- Barbrook AC, Santucci N, Plenderleith LJ, Hiller RG, Howe CJ. 2006. Comparative analysis of dinoflagellate chloroplast genomes reveals rRNA and tRNA genes. *BMC Genomics* 7:297.
- Barbrook AC, Symington H, Nisbet RER, Larkum A, Howe CJ. 2001. Organisation and expression of the plastid genome of the dinoflagellate Amphidinium operculatum. Mol Genet Genom. 266:632–638.
- Barbrook AC, Voolstra CR, Howe CJ. 2014. The chloroplast genome of a Symbiodinium sp clade C3 isolate. Protist 165:1–13.

- Bendtsen JD, Nielsen H, von Heijne G, Brunak S. 2004. Improved prediction of signal peptides: SignalP 3.0. J Mol Biol. 340:783–795.
- Bowler C, Allen AE, Badger JH, Grimwood J, Jabbari K, Kuo A, Maheswari U, Martens C, Maumus F, Otillar RP, et al. 2008. The *Phaeodactylum* genome reveals the evolutionary history of diatom genomes. *Nature* 456:239–244.
- Butterfield ER, Howe CJ, Nisbet RER. 2013. An analysis of dinoflagellate metabolism using EST data. *Protist* 164:218–236.
- Chen X, Kindle KL, Stern DB. 1995. The initiation codon determines the efficiency but not the site of translation initiation in *Chlamydomonas* chloroplasts. *Plant Cell* 7:1295–1305.

Crick FH. 1968. The origin of the genetic code. J Mol Biol. 38:367–379.

- Cummins CA, McInerney JO. 2011. A method for inferring the rate of evolution of homologous characters that can potentially improve phylogenetic inference, resolve deep divergence and correct systematic biases. *Syst Biol.* 60:833–844.
- Dang Y, Green BR. 2009. Substitutional editing of *Heterocapsa triquetra* chloroplast transcripts and a folding model for its divergent chloroplast 16S rRNA. *Gene* 442:73–80.
- de Vargas C, Audic S, Henry N, Decelle J, Mahé F, Logares R, Lara E, Berney C, Le Bescot N, Probert I, et al. 2015. Ocean plankton. Eukaryotic plankton diversity in the sunlit ocean. Science 348:1261605.
- Decelle J, Siano R, Probert I, Poirier C, Not F. 2014. Multiple microalgal partners in symbiosis with the acantharian *Acanthochiasma* sp. (Radiolaria). *Symbiosis* 58:233–244.
- Derelle E, Ferraz C, Rombauts S, Rouzé P, Worden AZ, Robbens S, Partensky F, Degroeve S, Echeynié S, Cooke R, et al. 2006. Genome analysis of the smallest free-living eukaryote Ostreococcus tauri unveils many unique features. Proc Natl Acad Sci USA. 103:11647–11652.
- Dorrell RG, Drew J, Nisbet RE, Howe CJ. 2014. Evolution of chloroplast transcript processing in *Plasmodium* and its chromerid algal relatives. *PLoS Genet.* 10:1004008.
- Dorrell RG, Hinksman GA, Howe CJ. 2016. Diversity of transcripts and transcript processing forms in plastids of the dinoflagellate alga *Karenia mikimotoi*. *Plant Mol Biol*. 90:233–247.
- Dorrell RG, Howe CJ. 2012. Functional remodeling of RNA processing in replacement chloroplasts by pathways retained from their predecessors. *Proc Natl Acad Sci USA*. 109:18879–18884.
- Dorrell RG, Howe CJ. 2015. Integration of plastids with their hosts: lessons learnt from dinoflagellates. *Proc Natl Acad Sci USA*. 112:10247–10254.
- Edgar RC. 2004. MUSCLE: multiple sequence alignment with high accuracy and high throughput. *Nucleic Acids Res.* 32:1792–1797.
- Emanuelsson O, Brunak S, von Heijne G, Nielsen H. 2007. Locating proteins in the cell using TargetP, SignalP and related tools. *Nat Protoc.* 2:953–971.
- Gavelis GS, White RA, Suttle CA, Keeling PJ, Leander BS. 2015. Single-cell transcriptomics using spliced leader PCR: evidence for multiple losses of photosynthesis in polykrikoid dinoflagellates. *BMC Genomics* 16:528.
- Gornik SG, Ford KL, Mulhern TD, Bacic A, McFadden GI, Waller RF. 2012. Loss of nucleosomal DNA condensation coincides with appearance of a novel nuclear protein in dinoflagellates. *Curr Biol.* 22:2303–2312.
- Gruber A, Rocap G, Kroth PG, Armbrust EV, Mock T. 2015. Plastid proteome prediction for diatoms and other algae with secondary plastids of the red lineage. *Plant J.* 81:519–528.
- Hallegraeff GM. 2010. Ocean climate change, phytoplankton community responses, and harmful algal blooms: a formidable predictive challenge. J Phycol. 46:220–235.
- Haxo FT, Kycia JH, Somers GF, Bennett A, Siegelman HW. 1976. Peridinin chlorophyll a proteins of dinoflagellate *Amphidinium carterae* (Plymouth 450). *Plant Physiol*. 57:297–303.
- Hiller RG. 2001. 'Empty' minicircles and petB/atpA and psbD/psbE (cytb(559) alpha) genes in tandem in Amphidinium carterae plastid DNA. FEBS Lett. 505:449–452.
- Hinder SL, Hays GC, Edwards M, Roberts EC, Waine AW, Gravenor MB. 2012. Changes in marine dinoflagellate and diatom abundance under climate change. *Nat Climate Change* 2:271–275.

- Hoppenrath M, Leander BS. 2010. Dinoflagellate phylogeny as inferred from heat shock protein 90 and ribosomal gene sequences. *PLoS One* 5:13220.
- Howe CJ, Nisbet RER, Barbrook AC. 2008. The remarkable chloroplast genome of dinoflagellates. J Exp Bot. 59:1035–1045.
- Huesgen PF, Alami M, Lange PF, Foster LJ, Schröder WP, Overall CM, Green BR. 2013. Proteomic amino-termini profiling reveals targeting information for protein import into complex plastids. *PLoS One* 8:74483.
- Hurst LD. 2002. The Ka/Ks ratio: diagnosing the form of sequence evolution. *Trends Genet.* 18:486.
- Inagaki Y, Simpson AGB, Dacks JB, Roger AJ. 2004. Phylogenetic artifacts can be caused by leucine, serine, and arginine codon usage heterogeneity: dinoflagellate plastid origins as a case study. *Syst Biol.* 53:582–593.
- Ishikawa SA, Inagaki Y, Hashimoto T. 2012. RY-Coding and nonhomogeneous models can ameliorate the maximum-likelihood inferences from nucleotide sequence data with parallel compositional heterogeneity. *Evol Bioinf.* 8:357–371.
- Janouskovec J, Horák A, Oborník M, Lukes J, Keeling PJ. 2010. A common red algal origin of the apicomplexan, dinoflagellate, and heterokont plastids. *Proc Natl Acad Sci USA*. 107:10949–10954.
- Janouskovec J, Sobotka R, Lai DH, Flegontov P, Koník P, Komenda J, Ali S, Prásil O, Pain A, Oborník M, et al. 2013. Split photosystem protein, linear-mapping topology, and growth of structural complexity in the plastid genome of *Chromera velia*. *Mol Biol Evol*. 30:2447–2462.
- Janouškovec J, Tikhonenkov D, Mikhailov K, Simdyanov T, Aleoshin V, Mylnikov A, Keeling P. 2013. Colponemids represent multiple ancient alveolate lineages. *Curr Biol.* 23:2546–2552.
- Kamiya N, Shen JR. 2003. Crystal structure of oxygen-evolving photosystem II from *Thermosynechococcus vulcanus* at 3.7-A resolution. *Proc Natl Acad Sci U S A*. 100:98–103.
- Kearse M, Moir R, Wilson A, Stones-Havas S, Cheung M, Sturrock S, Buxton S, Cooper A, Markowitz S, Duran C, et al. 2012. Geneious basic: an integrated and extendable desktop software platform for the organization and analysis of sequence data. *Bioinformatics* 28:1647–1649.
- Keeling PJ. 2010. The endosymbiotic origin, diversification and fate of plastids. *Phil Trans R Soc Biol Sci.* 365:729–748.
- Keeling PJ, Burki F, Wilcox HM, Allam B, Allen EE, Amaral-Zettler LA, Armbrust EV, Archibald JM, Bharti AK, Bell CJ, et al. 2014. The Marine Microbial Eukaryote Transcriptome Sequencing Project (MMETSP): illuminating the functional diversity of eukaryotic life in the oceans through transcriptome sequencing. *PLoS Biol.* 12:1001889.
- Kim S, Bachvaroff TR, Handy SM, Delwiche CF. 2011. Dynamics of actin evolution in dinoflagellates. *Mol Biol Evol*. 28:1469–1480.
- Kim SW, Jung WH, Ryu JM, Kim JB, Jang HW, Jo YB, Jung JK, Kim JH. 2008. Identification of an alternative translation initiation site for the *Pantoea ananatis* lycopene cyclase (*crtY*) gene in *E. coli* and its evolutionary conservation. *Protein Expr Purif.* 58:23–31.
- Lartillot N, Lepage T, Blanquart S. 2009. PhyloBayes 3: a Bayesian software package for phylogenetic reconstruction and molecular dating. *Bioinformatics* 25:2286–2288.
- Leterme SC, Seuront L, Edwards M. 2006. Differential contribution of diatoms and dinoflagellates to phytoplankton biomass in the NE Atlantic Ocean and the North Sea. *Mar Ecol Prog Ser.* 312:57–65.
- Lin S. 2011. Genomic understanding of dinoflagellates. *Res Microbiol.* 162:551–569.
- Miller MA, Schwartz T, Pickett BE, He S, Klem EB, Scheuermann RH, Passarotti M, Kaufman S, O'Leary MA. 2015. A RESTful API for access to phylogenetic tools via the CIPRES science gateway. *Evol Bioinform Online* 11:43–48.
- Moore RB, Obornik M, Janouskovec J, Chrudimsky T, Vancova M, Green DH, Wright SW, Davies NW, Bolch CJS, Heimann K, et al. 2008. A photosynthetic alveolate closely related to apicomplexan parasites. *Nature* 451:959–963.
- Morse D, Salois P, Markovic P, Hastings JW. 1995. A nuclear-encoded form II RuBisCO in dinoflagellates. *Science* 268:1622–1624.

- Moszczynski K, Mackiewicz P, Bodyl A. 2012. Evidence for horizontal gene transfer from Bacteroidetes bacteria to dinoflagellate minicircles. *Mol Biol Evol.* 29:887–892.
- Mungpakdee S, Shinzato C, Takeuchi T, Kawashima T, Koyanagi R, Hisata K, Tanaka M, Goto H, Fujie M, Lin S, et al. 2014. Massive gene transfer and extensive RNA editing of a symbiotic dinoflagellate plastid genome. *Genome Biol Evol.* 6:1408–1422.
- Nakamura Y. 1998. Growth and grazing of a large heterotrophic dinoflagellate, Noctiluca scintillans, in laboratory cultures. J Plankton Res. 20:1711–1720.
- Nassoury N, Morse D. 2005. Protein targeting to the chloroplasts of photosynthetic eukaryotes: getting there is half the fun. *Biochimic Biophys Acta* 1743:5–19.
- Nassoury N, Wang Y, Morse D. 2005. Brefeldin a inhibits circadian remodeling of chloroplast structure in the dinoflagellate gonyaulax. *Traffic* 6:548–561.
- Nelson MJ, Dang YK, Filek E, Zhang ZD, Yu VWC, Ishida K, Green BR. 2007. Identification and transcription of transfer RNA genes in dinoflagellate plastid minicircles. *Gene* 392:291–298.
- Nelson MJ, Green BR. 2005. Double hairpin elements and tandem repeats in the non-coding region of *Adenoides eludens* chloroplast gene minicircles. *Gene* 358:102–110.
- Nisbet RER, Koumandou VL, Barbrook AC, Howe CJ. 2004. Novel plastid gene minicircles in the dinoflagellate Amphidinium operculatum. Gene 331:141–147.
- Oudot-Le Secq MP, Grimwood J, Shapiro H, Armbrust EV, Bowler C, Green BR. 2007. Chloroplast genomes of the diatoms *Phaeodactylum tricornutum* and *Thalassiosira pseudonana*: comparison with other plastid genomes of the red lineage. *Mol Genet Genom*. 277:427–439.
- Pochon X, Putnam HM, Gates RD. 2014. Multi-gene analysis of *Symbiodinium* dinoflagellates: a perspective on rarity, symbiosis, and evolution. *Peer J.* 2:394.
- Probert I, Siano R, Poirier C, Decelle J, Biard T, Tuji A, Suzuki N, Not F. 2014. Brandtodinium gen. nov. and B. nutricula comb. nov. (Dinophyceae), a dinoflagellate commonly found in symbiosis with polycystine radiolarians. J Phycol. 50:388–399.
- Puthiyaveetil S, Kavanagh TA, Cain P, Sullivan JA, Newell CA, Gray JC, Robinson C, van der Giezen M, Rogers MB, Allen JF. 2008. The ancestral symbiont sensor kinase CSK links photosynthesis with gene expression in chloroplasts. Proc Natl Acad Sci U S A. 105:10061–10066.
- Reynolds JM, Bruns BU, Fitt WK, Schmidt GW. 2008. Enhanced photoprotection pathways in symbiotic dinoflagellates of shallow-water corals and other cnidarians. *Proc Natl Acad Sci U S A*. 105:13674–13678.
- Robbens S, Derelle E, Ferraz C, Wuyts J, Moreau H, Van de Peer Y. 2007. The complete chloroplast and mitochondrial DNA sequence of *Ostreococcus tauri*: organelle genomes of the smallest eukaryote are examples of compaction. *Mol Biol Evol.* 24:956–968.
- Ronquist F, Teslenko M, van der Mark P, Ayres DL, Darling A, Höhna S, Larget B, Liu L, Suchard MA, Huelsenbeck JP. 2012. MrBayes 3.2: efficient Bayesian phylogenetic inference and model choice across a large model space. *Syst Biol.* 61:539–542.
- Sato S, Nakamura Y, Kaneko T, Asamizu E, Tabata S. 1999. Complete structure of the chloroplast genome of *Arabidopsis thaliana*. DNA Res. 6:283–290.
- Ševčíková T, Horák A, Klimeš V, Zbránková V, Demir-Hilton E, Sudek S, Jenkins J, Schmutz J, Přibyl P, Fousek J, et al. 2015. Updating algal evolutionary relationships through plastid genome sequencing: did alveolate plastids emerge through endosymbiosis of an ochrophyte? *Sci Rep.* 5:10134.
- Shalchian-Tabrizi K, Skanseng M, Ronquist F, Klaveness D, Bachvaroff TR, Delwiche CF, Botnen A, Tengs T, Jakobsen KS. 2006. Heterotachy processes in rhodophyte-derived secondhand plastid genes: implications for addressing the origin and evolution of dinoflagellate plastids. *Mol Biol Evol.* 23:1504–1515.
- Siano R, Montresor M, Probert I, Not F, de Vargas C. 2010. Pelagodinium gen. nov. and P. béii comb. nov., a dinoflagellate symbiont of planktonic foraminifera. Protist 161:385–399.

- Stamatakis A. 2014. RAxML version 8: a tool for phylogenetic analysis and post-analysis of large phylogenies. *Bioinformatics* 30:1312–1313.
- Walker JE. 2013. The ATP synthase: the understood, the uncertain and the unknown. *Biochem Soc Trans.* 41:1–16.
- Wang D, Zhang Y, Zhang Z, Zhu J, Yu J. 2010. KaKs_Calculator 2.0: a toolkit incorporating gamma-series methods and sliding window strategies. *Genom Proteom Bioinf*. 8:77–80.
- Wang YL, Morse D. 2006. Rampant polyuridylylation of plastid gene transcripts in the dinoflagellate *Lingulodinium*. *Nucleic Acids Res.* 34:613–619.
- Wisecaver JH, Hackett JD. 2011. Dinoflagellate genome evolution. Ann Rev Microbiol. 65:369–387.
- Xia X. 2013. DAMBE5: a comprehensive software package for data analysis in molecular biology and evolution. *Mol Biol Evol.* 30: 1720–1728.

- Xia X, Xie Z, Salemi M, Chen L, Wang Y. 2003. An index of substitution saturation and its application. *Mol Phylogenet Evol.* 26:1–7.
- Yang Z. 2007. PAML 4: phylogenetic analysis by maximum likelihood. Mol Biol Evol. 24:1586–1591.
- Yang Z, Bielawski JP. 2000. Statistical methods for detecting molecular adaptation. *Trends Ecol Evol*. 15:496–503.
- Zauner S, Greilinger D, Laatsch T, Kowallik KV, Maier UG. 2004. Substitutional editing of transcripts from genes of cyanobacterial origin in the dinoflagellate *Ceratium horridum*. *FEBS Lett.* 577:535–538.
- Zhang H, Hou Y, Miranda L, Campbell DA, Sturm NR, Gaasterland T, Lin S. 2007. Spliced leader RNA transsplicing in dinoflagellates. *Proc Natl Acad Sci U S A*. 104: 4618-4623.
- Zhang Z, Green BR, Cavalier-Smith T. 1999. Single gene circles in dinoflagellate chloroplast genomes. *Nature* 400:155–159.